We are IntechOpen,
the world's leading publisher of
Open Access books
Built by scientists, for scientists

6,900
Open access books available

185,000
International authors and editors

200M
Downloads

154
Countries delivered to

Our authors are among the

TOP 1%
most cited scientists

12.2%
Contributors from top 500 universities

CLARIVATE ANALYTICS

BOOK CITATION INDEX

INDEXED

WEB OF SCIENCE™

Selection of our books indexed in the Book Citation Index
in Web of Science™ Core Collection (BKCI)

Interested in publishing with us?
Contact book.department@intechopen.com

Vanadium Redox Flow Batteries: Electrochemical Engineering

Sangwon Kim

Abstract

The importance of reliable energy storage system in large scale is increasing to replace fossil fuel power and nuclear power with renewable energy completely because of the fluctuation nature of renewable energy generation. The vanadium redox flow battery (VRFB) is one promising candidate in large-scale stationary energy storage system, which stores electric energy by changing the oxidation numbers of anolyte and catholyte through redox reaction. This chapter covers the basic principles of vanadium redox flow batteries, component technologies, flow configurations, operation strategies, and cost analysis. The thermodynamic analysis of the electrochemical reactions and the electrode reaction mechanisms in VRFB systems have been explained, and the analysis of VRFB performance according to the flow field and flow rate has been described. It is shown that the limiting current density of "flow-by" design is more than two times greater than that of "flow-through" design. In the cost analysis of 10 kW/120 kWh VRFB system, stack and electrolyte account for 40 and 32% of total cost, respectively.

Keywords: vanadium electrolyte, carbon electrode, overpotential, polarization, state of charge, flow-through, flow-by, flow rate, limiting current density, peak power density

1. Introduction

The global environmental is changing rapidly. The established world's first energy demand and biggest carbon emitter countries are being replaced by emerging countries. The use of renewable energy is expanding due to technological development and environmental problems. The global energy market is moving toward the reduction of fossil fuels and the expansion of environment friendly energy, a shift in the energy mix.

For stable supply of renewable energy with high volatility such as sunlight or wind power, securing stability of power system is the most important. To do this, an intelligent power network should be built up, and grid-based energy storage technology should be secured.

The vanadium redox flow battery is one of the most promising secondary batteries as a large-capacity energy storage device for storing renewable energy [1, 2, 4]. Recently, a safety issue has been arisen by frequent fire accident of a large-capacity energy storage system (ESS) using a lithium ion battery. The vanadium electrolyte is a nonflammable aqueous solution and has a high heat capacity to limit the temperature rise. Therefore, VRFB has no risk of ignition and explosion.

The power of VRFB depends on the performance of the stack, and the energy storage capacity depends on the electrolyte concentration and the electrolyte reservoir size, which greatly increases the degree of freedom in system design [7, 24]. A schematic diagram of the vanadium redox flow battery is shown in **Figure 1**.
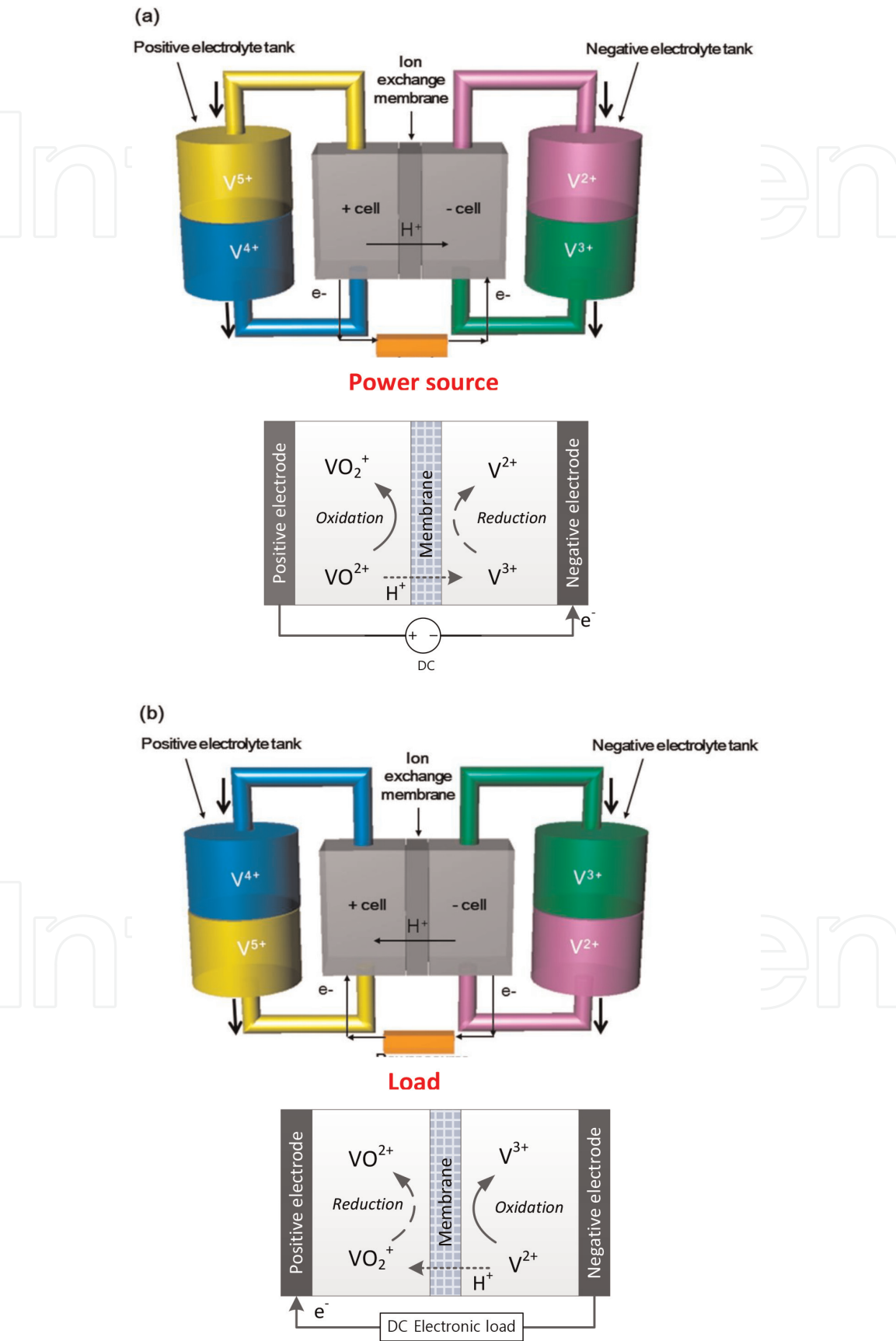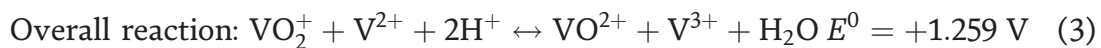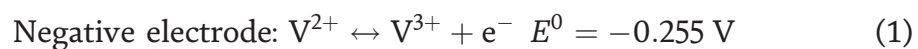

Figure 1.
Schematic of vanadium redox flow batteries: (a) charging and (b) discharging. Reproduced with permission from [3]. Copyright 2017 by Elsevier.

Flow batteries suffer from the capacity imbalance due to the mixing of the both side active materials caused by the electrolyte diffusion across the membrane, resulting in an irreversible loss of capacity as well as an efficiency loss [10–14]. Since the vanadium redox flow battery uses vanadium as the active material of both electrolytes, the use of appropriate rebalancing techniques can mitigate capacity loss though vanadium crossovers can lead to loss of efficiency.

2. Electrochemical reactions and kinetics

The vanadium ion may have various oxidation numbers from bivalent to pentavalent. Using this property, vanadium is used as the electrolyte redox couple material of the flow battery. VO_2^+, VO^{2+}, V^{3+}, and V^{2+} are represented by V(V), V(IV), V(III), and V(II) for explanation. Solution of V(III) is added to the negative electrolyte tank, and solution of V(IV) is added to the positive electrolyte tank as shown in **Figure 1**. When the electricity is applied to the electrodes, the V(III) ion of the negative electrolyte is reduced to V(II), and the V(IV) ion of the positive electrolyte is oxidized to V(V). This means that when the VRFB is charged, the difference in the oxidation number between the positive electrolyte and negative electrolyte increases from +1 to +3, and it can be under-stood conceptually that the electric energy is stored in the increased bivalent oxida-tion number. When the VRFB is discharged, V(II) in negative electrolyte is oxidized to V(III), and V(V) in positive electrolyte is reduced to V(IV). The chemical reactions for charge-discharge are expressed as follows:

$$\text{Negative electrode: } V^{2+} \leftrightarrow V^{3+} + e^- \quad E^0 = -0.255 \text{ V} \tag{1}$$

$$\text{Positive electrode: } VO_2^+ + e^- + 2H^+ \leftrightarrow VO^{2+} + H_2O \quad E^0 = +1.004 \text{ V} \tag{2}$$

$$\text{Overall reaction: } VO_2^+ + V^{2+} + 2H^+ \leftrightarrow VO^{2+} + V^{3+} + H_2O \quad E^0 = +1.259 \text{ V} \tag{3}$$
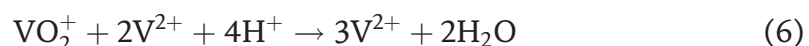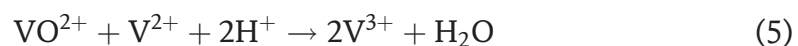
The permeation of the vanadium ions through the membrane occurs since any membrane cannot block the crossover of the redox species completely. The vanadium ions diffused to the counter electrode cause a cross-contamination reaction as below:
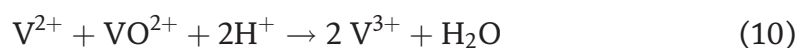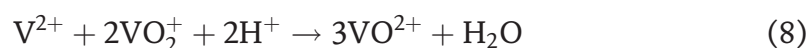
$$VO^{2+} + 2H^+ + e^- \leftrightarrow V^{3+} + H_2O \quad E^0 = +0.34 \text{ V} \tag{4}$$

The self-discharging reactions caused by the vanadium ions permeated into the counter electrolytes can be described as below:
Negative electrode:

$$VO^{2+} + V^{2+} + 2H^+ \rightarrow 2V^{3+} + H_2O \tag{5}$$

$$VO_2^+ + 2V^{2+} + 4H^+ \rightarrow 3V^{2+} + 2H_2O \tag{6}$$

$$VO_2^+ + V^{3+} \rightarrow 2\,VO^{2+} \tag{7}$$

Positive electrode:

$$V^{2+} + 2VO_2^+ + 2H^+ \rightarrow 3VO^{2+} + H_2O \tag{8}$$

$$V^{3+} + VO_2^+ \rightarrow 2\,VO^{2+} \tag{9}$$

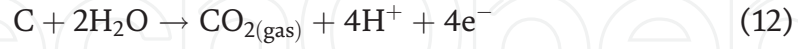$$V^{2+} + VO^{2+} + 2H^+ \rightarrow 2\,V^{3+} + H_2O \tag{10}$$

When the VRFB is overcharged, hydrogen and oxygen gas can be generated at the negative and positive electrodes, respectively. Additionally, the carbon dioxide gas can be generated by corrosion of graphite plate with the produced oxygen gas.

Negative electrode:

$$2H^+ + 2e^- \rightarrow H_{2(gas)} \tag{11}$$

Positive electrode:

$$C + 2H_2O \rightarrow CO_{2(gas)} + 4H^+ + 4e^- \tag{12}$$

$$2H_2O \rightarrow O_{2(gas)} + 4H^+ + 4e^- \tag{13}$$

$$C + O_{2(gas)} \rightarrow CO_{2(gas)} \tag{14}$$

The equilibrium cell potentials, E_{eq} for each reaction, are calculated using Nernst equation according to

$$E_{eq,\,neg} = E^0_{neg} + \frac{RT}{F} ln\left(\frac{C_{V^{3+}}}{C_{V^{2+}}}\right) \tag{15}$$

$$E_{eq,\,pos} = E^0_{pos} + \frac{RT}{F} ln\left(\frac{C_{VO_2^+}(c_{H^+})^2}{C_{VO^{2+}}}\right) \tag{16}$$

$$E_{eq,\,overall} = E^0_{overall} + \frac{RT}{F} ln\left(\frac{C_{VO_2^+}(C_{H^+})^2}{C_{VO^{2+}}}\frac{C_{V^{2+}}}{C_{V^{3+}}}\right) \tag{17}$$

where $C_i{}^*$ is the concentration of the i species; E^0 is the standard cell potential for the electrode reaction; R is the ideal gas constant, 8.314 J/mol K; T is the cell temperature; and F is Faraday's constant, 96,485 As/mol.

The exchange current density is the magnitude of the current when the electrode reactions reach the equilibrium and can be described as

$$i_{0,\,neg} = Fk^0_{neg} C_{V^{3+}}^{*\left(1-\alpha_{neg}\right)} C_{V^{2+}}^{*\,\alpha_{neg}} \tag{18}$$

$$i_{0,\,pos} = Fk^0_{pos} C_{VO_2^+}^{*\left(1-\alpha_{pos}\right)} C_{VO^{2+}}^{*\,\alpha_{pos}} \tag{19}$$

where k^0 is the standard rate constant.

Following the Butler-Volmer equation [5, 24], the currents at negative electrode and positive electrode are described as

$$i_{neg} = i_{0,\,neg} \left[\left(\frac{C_{V^{3+}}(0,t)}{C_{V^{3+}}^*}\right) \exp\left(-\frac{\alpha_{neg}F}{RT}\eta_{neg}\right) - \left(\frac{C_{V^{2+}}(0,t)}{C_{V^{2+}}^*}\right) \exp\left(\frac{(1-\alpha_{neg})F}{RT}\eta_{neg}\right)\right] \tag{20}$$

$$i_{pos} = i_{0,\,pos} \left[\left(\frac{C_{VO_2^+}(0,t)}{C_{VO_2^+}^*}\right) \exp\left(-\frac{\alpha_{pos}F}{RT}\eta_{pos}\right) - \left(\frac{C_{VO^{2+}}(0,t)}{C_{VO^{2+}}^*}\right) \exp\left(\frac{(1-\alpha_{pos})F}{RT}\eta_{pos}\right)\right] \tag{21}$$

where α is the transfer coefficient or symmetry factor and η is the overpotential, defined as $\eta = \phi_s - \phi_l - E_{eq}$.

where φ_s is the electric potential of the solid electrode and φ_l is the electrolyte potential.

The standard open-circuit voltage of VRFB, $E^0 = 1.26$ V, can be derived from Gibbs free energy relation as below:

$$\Delta G^0 = \Delta H^0 - T\Delta S^0 = -nFE^0 = -119.3 \ kJ/mol \tag{22}$$

However, the actual operating voltage of VRFB differs from this thermodynamic value. Charging voltage should be larger than 1.26 V since the amount of overpotential is required in addition to the thermodynamic voltage. **Figure 2** shows the relationship of the voltage and current during charging and discharging at the two electrodes of VRFB, assuming that the overall kinetics are determined by the charge transfer in the electrochemical reaction.

$$E_{charge} = E^0_{cell} + \eta_a + \eta_c + iR_{total} \tag{23}$$

$$E_{discharge} = E^0_{cell} - \eta_a - \eta_c - iR_{total} \tag{24}$$

where η_a is anodic overpotential and η_c is cathodic overpotential.

At discharge, the operating voltage becomes smaller than theoretical value. As the current density increases, the overpotential and iR drop increase, so the charging voltage increases and the discharging voltage decreases as shown in **Figure 3c**. Energy density and power density can be calculated in Eqs. (25) and (26), respectively.

$$\text{Energy density} = \frac{nCFV_{dis}}{N_{tank}} = \frac{1 \times \frac{1.6mol}{L} \times 26.8 \frac{Ah}{mol} \times 1.3 \ V}{2} = 27.872 \ Wh/L \tag{25}$$

$$\text{Power denisty} = \text{current density} \times \overline{V}_{discharge} \tag{26}$$

where n is the number of electrons transferred during reactions, C is a vanadium electrolyte concentration, 1.6 mol/L, $\overline{V}_{discharge}$ is averaged discharge voltage, and
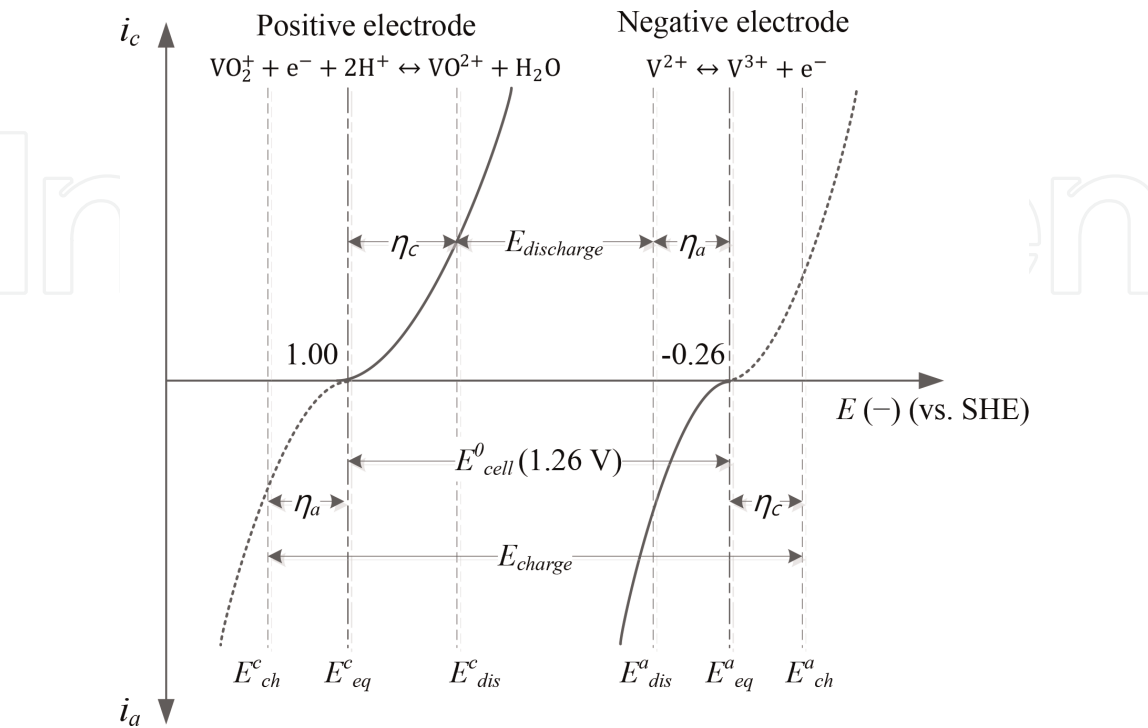

Figure 2.
Charge-discharge voltage of vanadium redox flow battery: Current vs. voltage and overpotential and open-circuit voltage at positive electrode and negative electrode.
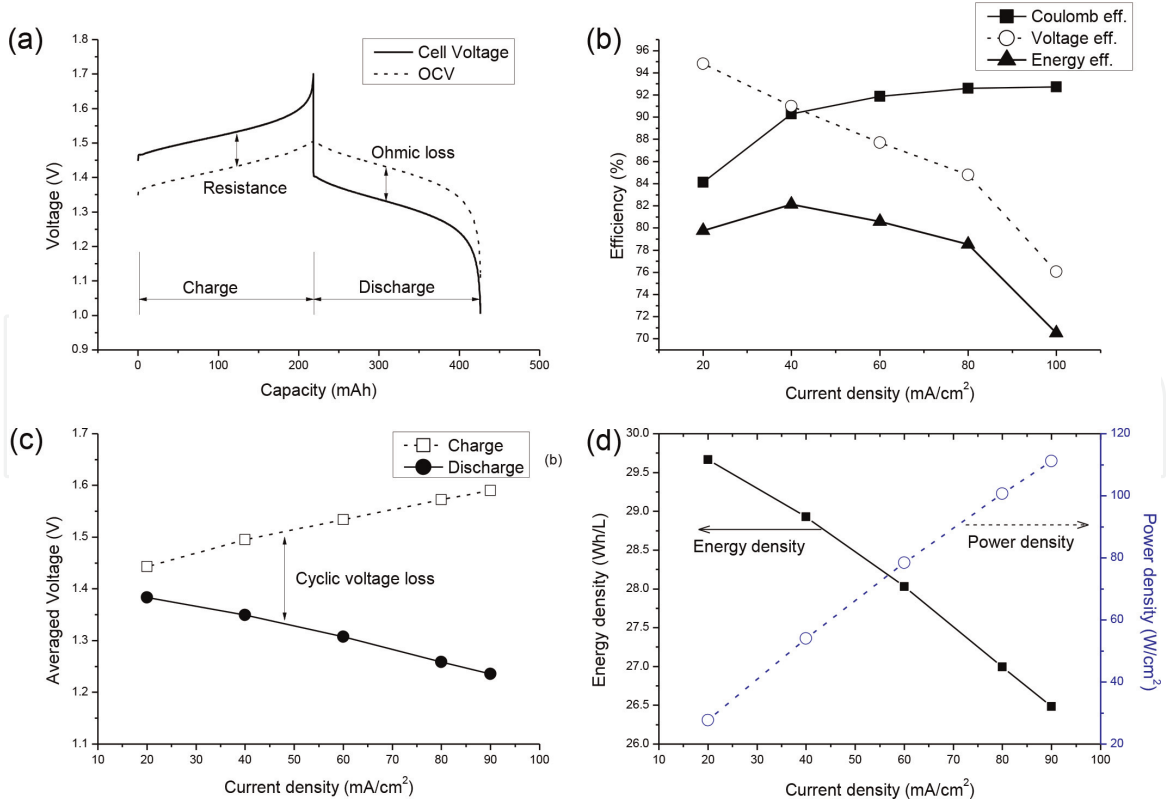
Figure 3.
Vanadium redox flow battery performance: (a) cell voltage and open-circuit voltage profiles at current density of 60 mA/cm², (b) efficiencies depending on current densities, (c) polarization plot of the unit cell, and (d) energy density and power density.

N_{tank} is a number of tank. There are only three variables that contribute to increasing energy density and power density: the vanadium ion concentration, discharging voltage, and current density. However, the concentration of the vanadium ions is limited by low solubilities of vanadium ions in aqueous solution. The discharging voltage and current density are restricted by the electrochemical activities of vanadium electrolyte. **Figure 3d** shows that as a current density increases, energy density decreases, and power density increases. Normal operating current density range is 50–80 mA/cm², and stored energy density is in the range of 25–35 Wh/L or 20–32 Wh/kg. The corresponding power density is less than 0.1 W/cm².

The performance of VRFB can be measured with three efficiencies: current efficiency, voltage efficiency, and energy efficiency, which are defined in Eqs. (27), (28), and (29), respectively. The current efficiency (CE, Coulombic efficiency) is defined as the ratio of the amount of usable charge to the stored charge amount, that is, the discharge capacity divided by the charge capacity. CE is a measure of the storage capacity loss during charge-discharge process. The capacity loss is mainly caused by the crossover of the electrolyte ions through the membrane. The mixed active materials result in a capacity imbalance between the anode and cathode electrolytes and an irreversible capacity loss.

$$CE = \frac{discharge\ capacity}{charge\ capacity} \times 100\% = \frac{\int_{dis} I(t)dt}{\int_{ch} I(t)dt} \times 100\% = \frac{I_{dis} \bullet t_{dis}}{I_{ch} \bullet t_{ch}} \times 100\%$$
$$= \frac{t_{dis}}{t_{ch}} \times 100\% (\text{If } I_{dis} = I_{ch}) \tag{27}$$

$$VE = \frac{average\ discharge\ voltage}{average\ charge\ voltage} \times 100\% = \frac{\int_{dis} V(t)dt \big/ t_{dis}}{\int_{ch} V(t)dt \big/ t_{ch}} \times 100\% \tag{28}$$

$$EE = \frac{discharge\ energy\ (Wh)}{charge\ energy\ (Wh)} \times 100\% = \frac{\int_{dis} I(t)V(t)dt}{\int_{ch} I(t)V(t)dt} \times 100\%$$

$$= \frac{I_{dis} \bullet t_{dis}}{I_{ch} \bullet t_{ch}} \frac{\int_{dis} V(t)dt / t_{dis}}{\int_{ch} V(t)dt / t_{ch}} \times 100\% = CE \times VE \tag{29}$$

Voltage efficiency (VE) is the average discharge voltage to the average charge voltage. **Figure 3a** shows the charging and discharging curves of VRFB in constant current mode, in which the current is maintained as constant value during charge-discharge cycle. While the current is constant during charge-discharge, the voltage is not constant but gradually changing in the whole cycle. Voltage efficiency represents a measure of electrical resistance loss and the polarization properties of battery. The polarization plot in **Figure 3c** coincides with the voltage efficiency trend in **Figure 3b**. Energy efficiency is the ratio of available energy to stored energy, which can be calculated as the product of voltage efficiency and current efficiency.

It is important to monitor the charging status of VRFB since especially overcharging the battery results in gas evolution side reactions, cell resistance increase, and capacity loss. Normally, VRFB is operated in charge range of 20–80%. The status of charge (SOC) is defined as the following using the concentrations of vanadium ions [8, 9]:

$$SOC = \frac{C_{V^{2+}}}{C_{V^{2+}} + C_{V^{3+}}} = \frac{C_{VO_2^+}}{C_{VO_2^+} + C_{VO^{2+}}} \tag{30}$$

3. Electrode

The electrode provides the active sites for the redox reaction of redox couples dissolved in the electrolyte notwithstanding the electrode itself does not participate in the reaction. The electrode material influences the performance of VRFB diversely. The electrode should be electrochemically stable in the operating potential window of VRFB. The electrochemical activity of electrode affects the charge-discharge voltages and consequently the voltage efficiency during battery cycle operation. The electrode must have high electrical conductivity to increase the charge transfer speed. The charge transfer speed is related the ohmic losses, cell voltage, and energy efficiency. The vanadium can be dissolved in strong acidic aqueous solution; therefore the electrode should be chemically stable in strong acidic condition. The chemical stability of the electrode in acid electrolyte is related to the corrosion resistance when oxygen is generated at the positive electrode during overcharged and determines the lifetime of VRFB. The porosity of the electrode affects the pumping energy loss, which affects pressure drop across the stack and overall battery system efficiency [15, 16].

3.1 Reaction mechanism at carbon felt electrode

Various carbon materials including carbon felt, graphite felt, and carbon paper have been extensively studied as electrodes for VRFB. Especially, carbon felts are considered to be suitable for use as electrodes of VRFB because of their wide specific surface area, high electrical conductivity, high chemical stability, and wide operating potential window.

Sun and Skyllas-Kazacos reported that the C-OH functional group acts as an active site for oxidation of VO^{2+} and reduction of V^{3+} on the surface of the electrode [17, 18]. Oxidation and reduction mechanisms of the VO_2^+/VO^{2+} and V^{2+}/V^{3+}

redox couples at the electrode surface can be explained in three steps as shown in **Figure 4**. At first step of charge process, the vanadium ions are diffused from the bulk electrolytes to the vicinity of the electrodes and absorbed on the surface of the electrodes. The absorbed vanadium ions are connected to the electrode through the exchange with functional group hydrogen ions. In the second step, the electron and oxygen transfer reactions occur in the VO_2^+/VO^{2+} redox couple, and only the electron transfer reaction occurs in the V^{2+}/V^{3+} redox couple. At the positive electrode, an oxygen atom of C-O functional group moves to the VO^{2+}, and an electron of the VO^{2+} is transferred to the electrode following the C-O-V bond, and the oxidation number of vanadium ion increases from +4 to +5. At the negative electrode, an electron is transferred from the electrode to the V^{3+} along the C-O-V
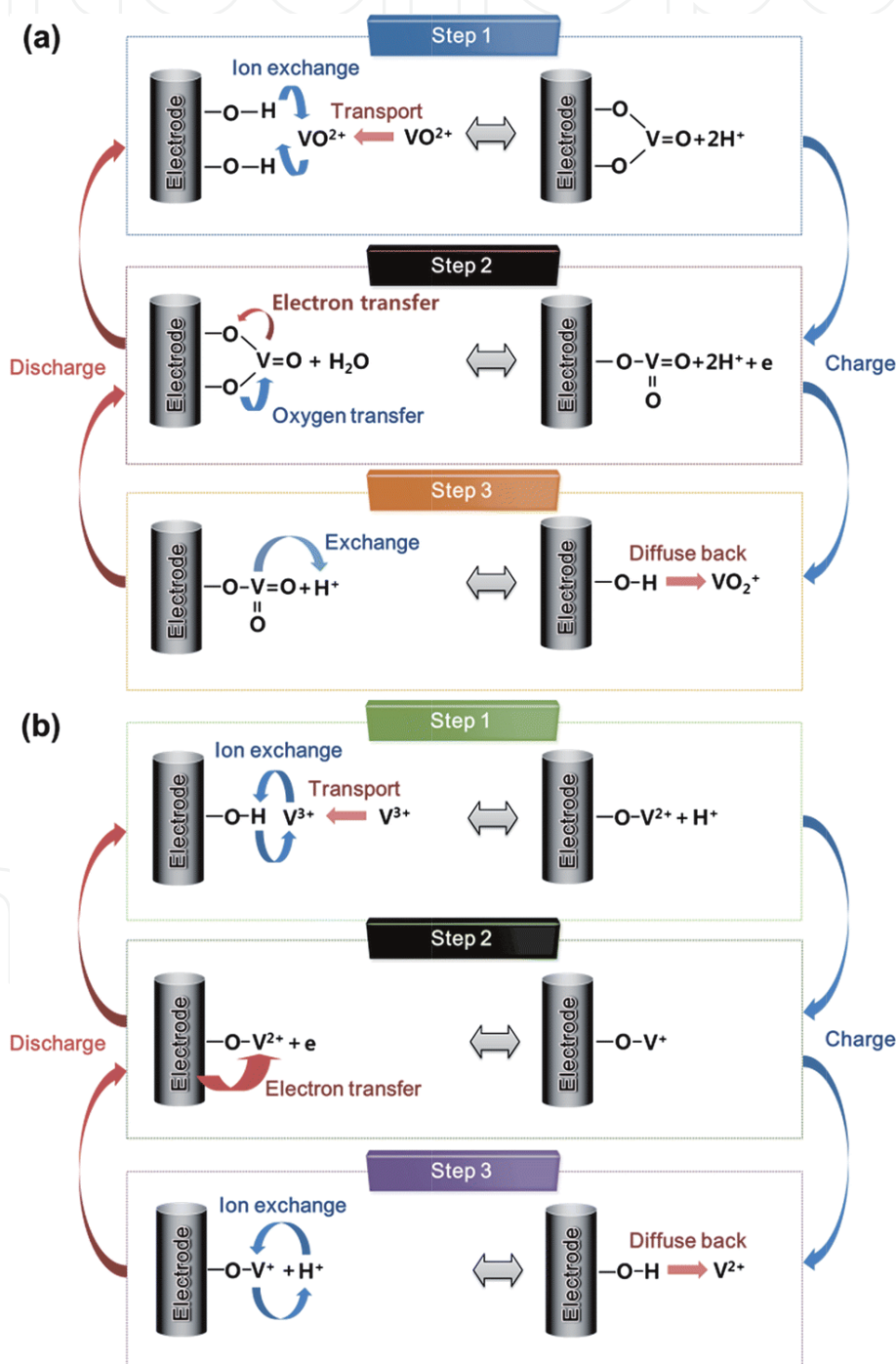

Figure 4.
Schematic illustration of the redox reaction mechanism for (a) VO_2^+/VO^{2+} redox couples in the catholyte and (b) V^{2+}/V^{3+} redox couple in the anolyte on the surface of the carbon felt electrode in VRFB. Reproduced with permission from [16]. Copyright 2015 by the Royal Society of Chemistry.

bond, and the oxidation number of vanadium ion is reduced from +3 to +2. In the third step, the ion exchange process between the V ion attached to the electrode surface and the H^+ ion in the electrolyte occurs, and the produced reactants (VO_2^+ and V^{2+}) diffuse back into the originated electrolytes, respectively.

To improve the electrochemical performance of VRFB, it is necessary to promote the reaction kinetics of vanadium ion redox couples. For this purpose, the electrode should have high electrical conductivity and the sufficient amount of oxygen and nitrogen functional groups at the surface.

3.2 Electrochemical characters

Cyclic voltammetry (CV) is used to monitor the reaction rates of redox couples and to evaluate the electrode performance of flow batteries. The CV curves in **Figure 5** show the electrode characteristics of the VRFB cell. The negative potential region of CV indicates the redox reaction of V^{2+}/V^{3+} ions, and the positive potential region implies the redox reaction of VO_2^+/VO^{2+} ions in electrolyte.

Figure 5a compares the electrode characteristics of the standard sulfuric acid electrolyte and the mixed acid electrolyte containing 6 M Cl^-. The peak current of the vanadium redox reaction is higher in the mixed electrolyte than in the standard sulfuric acid solution. This indicates that the reaction kinetics is improved due to the excellent fluidity of the electrolyte by adding sulfate chloride. The reaction voltage of the redox couples in the mixed solution increases slightly comparing to the sulfate solution, but there is no significant difference in the electrochemical reversibility between the sulfuric acid and the mixed electrolyte.

Figure 5b shows the reaction characteristics of carbon paper and catalytic behavior of biomass-derived activated carbon (AC) in the vanadium electrolyte. The V^{3+}/VO^{2+} redox couple peaks appear clearly in AC-coated carbon paper CV curve, and these multivalent peaks reveal the superior catalytic activity of AC coating.

Park et al. [21] investigated the change of VRFB performance according to the compression ratio of the carbon felt electrode and suggested the optimal compression ratio of the electrode. Oh et al. [22] conducted a numerical study of the VRFB model to investigate the effect of electrode compression on the charging and discharging behavior of VRFB. Yoon et al. [23] studied the flow distribution depending on local porosity of the electrode both numerically and experimentally.
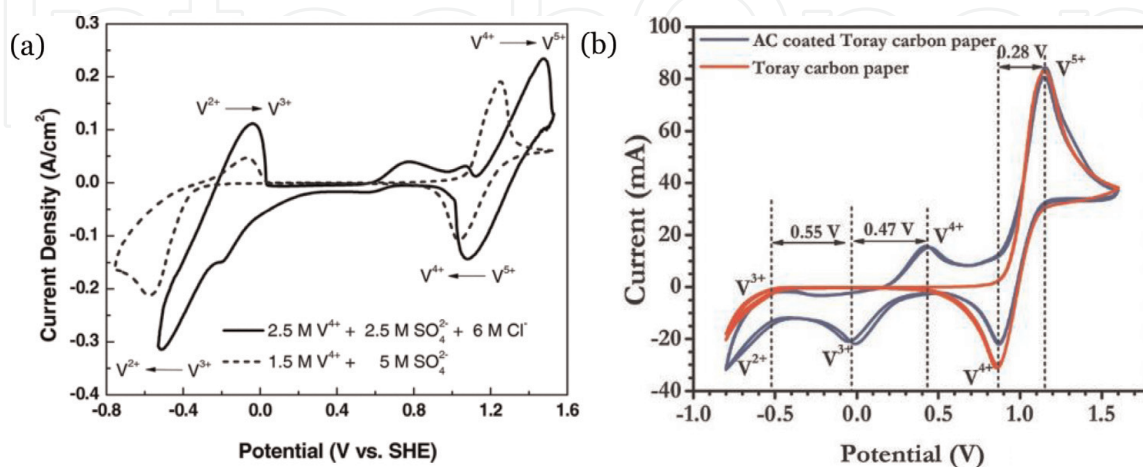

Figure 5.
(a) Cyclic voltammograms on a graphite felt electrode of a standard sulfate VRFB electrolyte (1.5 M V^{4+} and 5.0 M SO_4^{2-}) and a mixed electrolyte solution (2.5 M V^{4+}, 2.5 M SO_4^{2-}, and 6 M Cl^-) at a scan rate of 0.5 mV/s. Reproduced with permission with [19]. Copyright 2011 Wiley. (b) Cyclic voltammograms on Toray carbon sheets with and without mesoporous AC loading in the presence of 1.7 M $V^{3.5+}$ in 4 M H_2SO_4 solutions at a scan rate of 5 mV/s. Reproduced with permission from [20]. Copyright 2015 Elsevier.
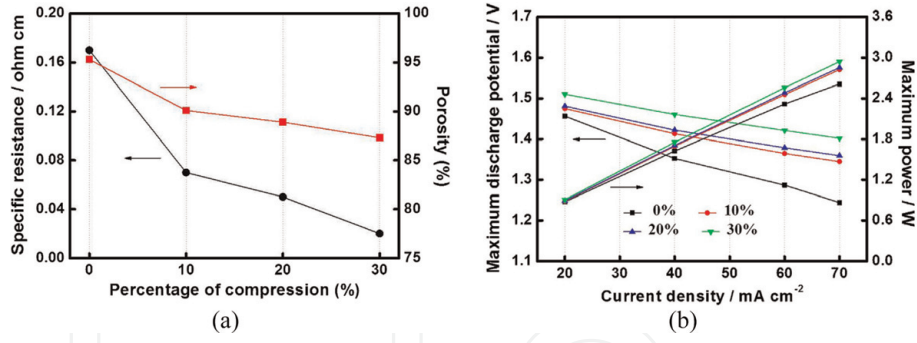
Figure 6.
(a) Specific resistance and porosity vs. percentage of compression for FA-30A carbon felt electrodes and (b) polarization curves of VRFB cells with electrodes of various levels of compression. Reproduced with permission from [21]. Copyright 2014 Elsevier.

As the percentage of electrode compression increases, the specific resistance and porosity of the electrode decrease as shown in **Figure 6a**. Compressed electrodes with reduced resistivity promote electron transfer, which increases the discharge time and maximum power of the VRFB cell and significantly increases VRFB performance efficiencies and discharge capacities, especially under high current density (**Figure 6b**). However, decreased porosity reduces the electrolyte flow passages through the electrode and increases pumping losses. The energy efficiency of the battery increases with increasing electrode compression ratio of up to 20%. When the carbon felt electrode is compressed more than 20%, the energy efficiency can be reduced due to the combined effect of deteriorated electrolyte transport and enhanced electron transfer. Overall, it can be concluded that the compression of the carbon felt electrode has a positive effect on cell performance, and the compression ratio optimization can generate significant improvement of VRFB performance without additional cost.

4. Electrolyte flow

The flow characteristics have a significant effect on the performance of redox flow battery. The flow distribution is related to the supply of reactant and participation of active species in redox reaction. The uniform flow distribution represents the uniform current density distribution. If the electrolyte flows nonuniformly, the reactants are not fully employed to the electrochemical reaction, which will lead to the degradation of the VRFB performance and durability.

Electrolyte flow rate is the speed of supplying reactants to the active site of electrode. If the flow rate is not enough, the capacity of the electrolytes is not fully utilized. If the flow rate is too high, the pumping loss increases, and the overall system efficiency is reduced accordingly. Therefore, optimizing flow rate is necessary in VRFB operation, and the importance increases significantly as storing capacity increases. The theoretical flow rate can be calculated as below [8]:

$$Q_{theo} = \frac{I}{n \times F \times C \times SOC_{min}} \tag{31}$$

where I is the current; n is the number of electrons transferred during the reaction, which is 1 for VFB; C is the total vanadium concentration for each reservoir (1.6 M); and SOC_{min} is the minimum state of charge, which is 20% normally.

The stoichiometric number, λ, is defined as the ratio of the actual flow rate to theoretical flow rate. **Figure 7** shows that as the stoichiometric number increases, the charge-discharge cycle time increases. The extension of the cycle time can be
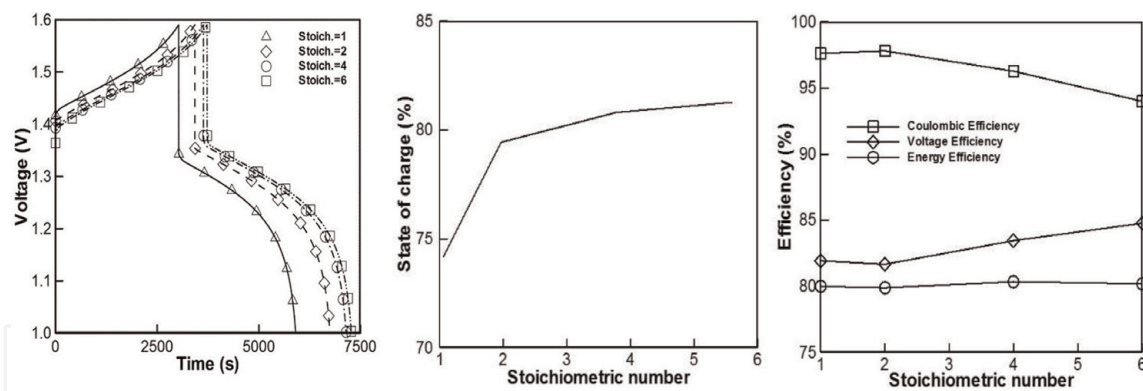
Figure 7.
Current density of 75 mA/cm² at various flow rates; (a) charge–discharge curve, (b) SOC, and (c) efficiencies as a function of stoichiometric number ($\lambda = Q_{real}/Q_{theo}$). Reproduced with permission from [8]. Copyright 2018 Elsevier.

explained as the increase in capacity of the VRFB, which means that the battery can store more energy. **Figure 7b** shows SOC increasing corresponding to the flow rate increase. On this basis, it is clear that a large mass flow rate can enhance the utilization of vanadium ions. This result explains the increase in the VFB capacity as the stoichiometric number increases. The variation of the efficiencies according to the flow rate is shown in **Figure 7c** and similar to the efficiency behavior according to the current density.

Flow patterns of RFB can be categorized into two types: "flow-through" type without flow field and "flow-by" type which has a flow field design on the bipolar plate. Leung et al. [25] explained that the structure in which the flow direction is parallel to the current direction is "flow-through" type and the structure in which the flow direction is perpendicular to the current direction is "flow-by" type. However, this definition does not match the concept we are dealing with here. In the scheme described here, the directions of electrolyte flow and electric current are perpendicular to each other in both "flow-through" and "flow-by" configurations. **Figure 8** shows the flow battery stack configuration and conceptual schematics of both flow designs. The classical "flow-through" type is the configuration in which the electrolyte flows through the porous carbon felt electrode. A "flow-by" type is the structure in which the electrolyte flows by the surface of an electrode following the flow field at the bipolar plate like a fuel cell. A "flow-by" type can choose relatively thinner carbon felt or carbon paper as an electrode material. Zawodzinski's group first reported better electrochemical performance and improved limiting current density and peak power density of VRFB with a "zero-gap" serpentine flow field design comparing to "flow-through" configuration [29]. This results from reduced ohmic loss and enhanced localized mass transfer due to thinner thickness and larger surface area-to-volume ratio of carbon paper used as electrode than those of carbon felt. Elgammal et al. [30] achieved normalized limiting current density of 2961 mA/cm² mol and peak power density of 2588 mW/cm² of VRFB with serpentine flow field. However, "flow-through" configuration distributes the electrolyte flow more uniformly and results in less pressure drops and pumping losses than "flow-by" configuration.

The electrolyte flow behavior is indicated schematically in **Figure 9**. The electrolyte is flowing mainly following channel over the electrode and partly penetrating into the porous electrode forced by pressure gradient. The flow velocity through the porous carbon media is lower than mean velocity of fully developed channel flow. The amount of the electrolyte penetrated into the porous electrode is associated with the stoichiometric availability of electrolyte reactants and the battery performance.
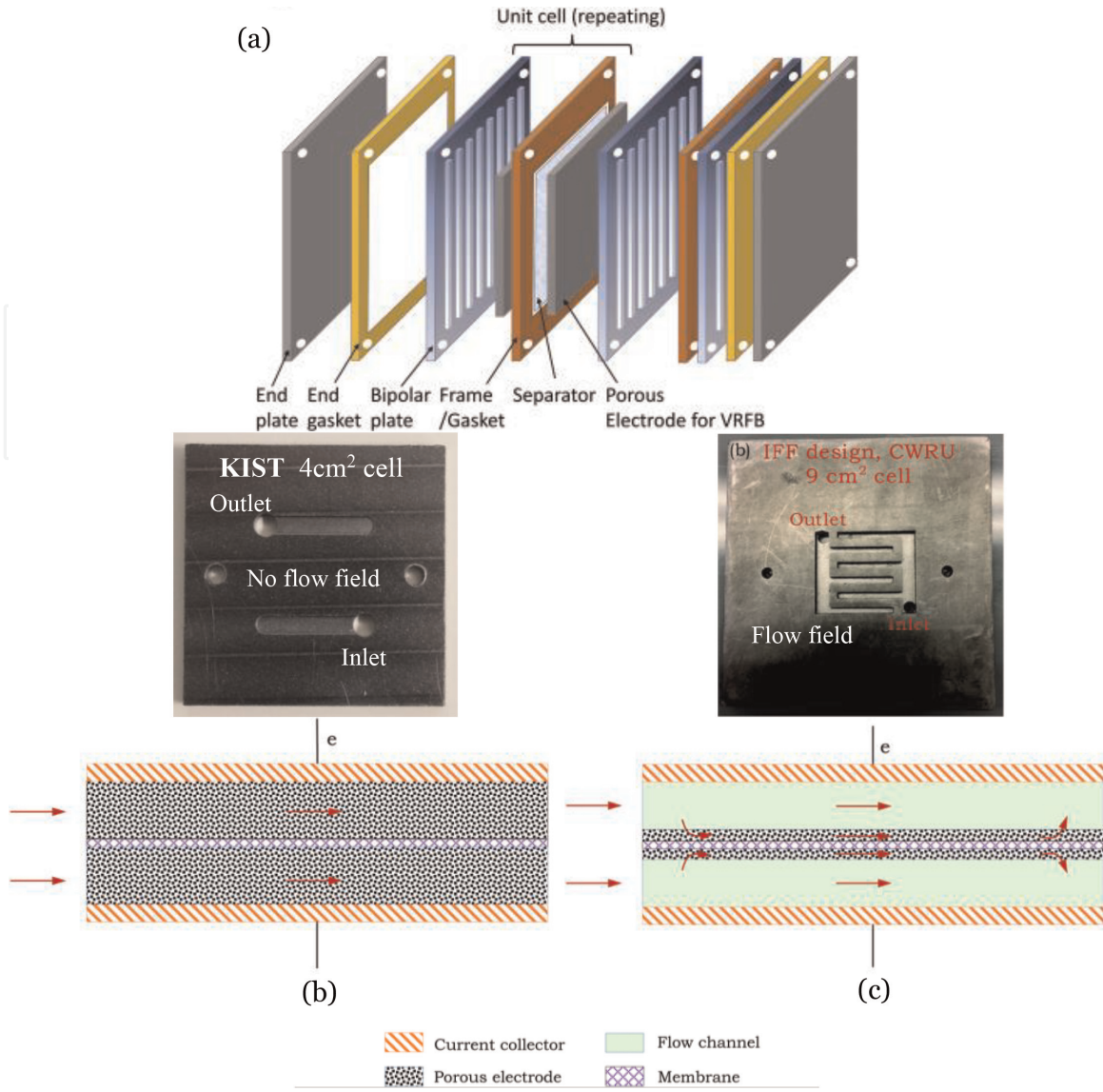
Figure 8.
(a) Schematic of flow battery stack configuration. Reproduced with permission from [31]. Copyright 2015 by Elsevier. (b) Bipolar plate and two-dimensional configuration of "flow-through" design and (c) "flow-by" design. Reproduced with permission from [26]. Copyright 2018 by the Royal Society of Chemistry.

Limiting current density is a key factor evaluating flow battery performance. High current density allows fast electrochemical reactions and reduces charging time. Newman et al. developed the limiting current density model as below [6]:

$$i_{lim} = 0.9783 \frac{nFDc}{L} \int_{0}^{L} \left(\frac{u_f}{hDX} \right)^{\frac{1}{3}} dX \qquad (32)$$

where n is the number of electrons transferred during reactions, D is the diffusion coefficient, c is the bulk electrolyte concentration, L is the length of the flow channel, u_f is the averaged electrolyte flow velocity along the flow channel, and h is the distance between one electrode and one flat plate. Newman's model predicts the limiting current density of an electrolyte flowing between one flat plate and one electrode as shown in **Figure 9c** assuming no electrolyte penetration into the electrode surface.

The limiting current density dominated by the stoichiometric availability of reactant in the porous electrode as shown in **Figure 9d** is called "maximum current density" and can be expressed in Eq. (33) [26, 27]:
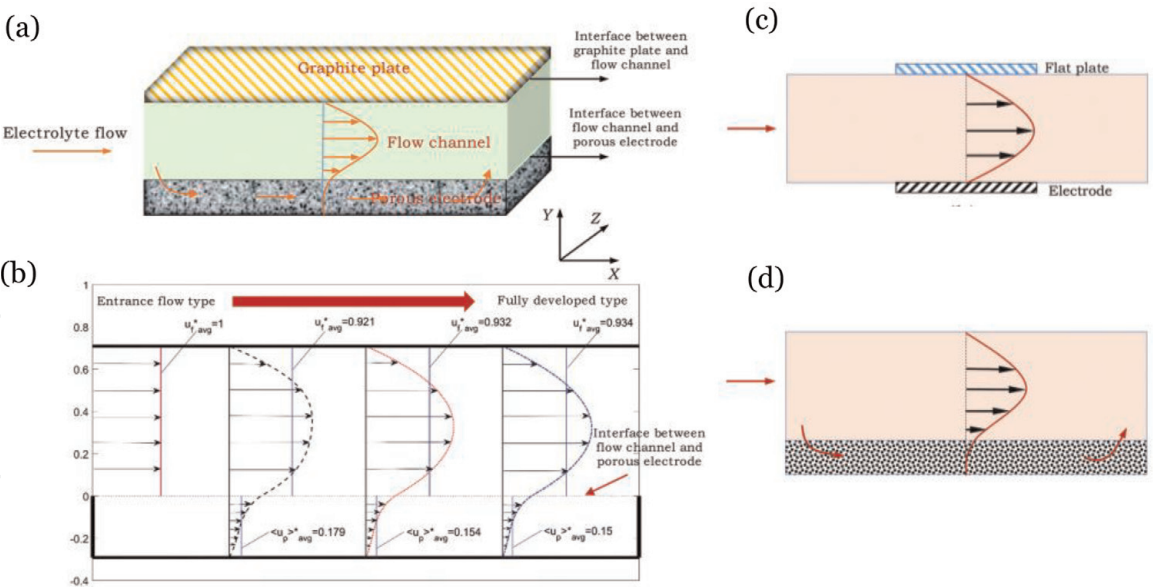
Figure 9.
(a) Diagram of electrolyte flow through a single flow channel and over the porous electrode in RFBs, (b) two-dimensional flow distributions in the flow channel-porous electrode layered system, and (c) the case of current density limited by the diffusion boundary layer formed between one flat plate and one electrode, which does not allow electrolyte reactant penetration. (d) the case of current density limited by the stoichiometric availability of the electrolyte reactants penetrate through the porous electrode from the flow channel. Reproduced with permission from [26]. Copyright 2018 by the Royal Society of Chemistry.

$$i_{max} = \frac{nFcQ_p}{A} \tag{33}$$

where Q_p is the volumetric flow of electrolyte reactant penetration through the interface between the flow channel and porous electrode and A is the cross-section area of porous electrode that is perpendicular to the current direction.

The entrance flow rate of "flow-by" type is higher than "flow-through" type. If entrance flow rate is increased, the penetrating electrolyte flow into the porous electrode is increased because the diffusion boundary layer is decreased, and the maximum current density is increased according to Eq. (33).

Zawodzinski et al. have shown how the discharge polarization curves of VRFB behave with the flow field and flow rate variations [28]. The flow-through type shows a limiting current density of 165 mA/cm^2 at an electrolyte circulation rate of 30 ml/min
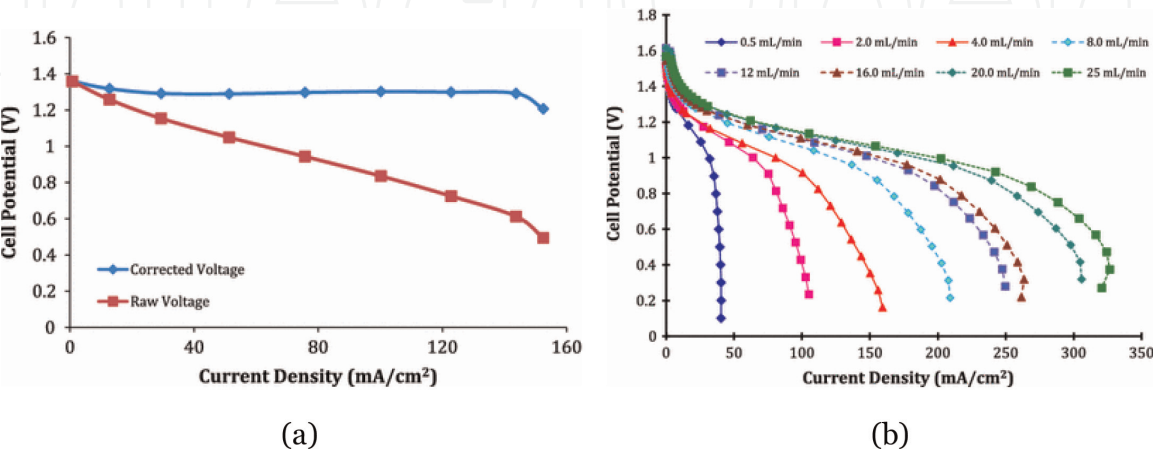

Figure 10.
(a) Discharging polarization curve of the flow-through type VRFB (0.5 M V/2.0 M H_2SO_4 electrolyte with 30 ml/min) and (b) iR free discharge polarization curves illustrating the effect of the electrolyte flow rate on flow-by type VRFB (1.0 M V/5.0 M H_2SO_4 electrolyte). Reproduced with permission from [28]. Copyright 2011 by springer.

Flow rate (ml/min)	Theoretical limiting current density (mA/cm^2)	Observed limiting current density (mA/cm^2)	Percent of max current
0.5	161	40	25.2
2	643	105	16.3
4	1287	159	12.4
8	2573	209	8.12
12	3860	250	6.48
16	5147	261	5.07
20	6433	306	4.76
25	8042	321	3.99

Table 1.
Comparison of theoretical limiting current density and observed current density in flow-by configuration of VRFB at various electrolyte flow rates. Reproduced with permission from [28]. Copyright 2011 by springer.

(**Figure 10a**). **Figure 10b** shows that the limiting current density of the flow-by type increases from 40 to 321 mA/cm^2 as the flow rate increases from 0.5 to 25 ml/min. The values of the theoretical and observed limit current density according to the flow rate are summarized in **Table 1**. The theoretical limiting current density was calculated by converting the transfer rate of the electrolyte to the bipolar plate into the number of available electrons, assuming that all vanadium was converted in a single pass.

5. Cost analysis

Various batteries compete to become renewable energy storage devices in the power grid. One of the most important factors in practical implementation is the battery installation cost (capital cost). Noack et al. [32] conducted a techno-economic modeling analysis based on a 10 kW/120 kWh VRFB system. The costs and ratios of each component are summarized in **Table 2** and **Figure 11,** respectively. The largest portion of the VRFB cost is the stack, which accounts for 40% of

VRFB system parameter	Cost	VRFB stack component	Cost
Electrolyte	€ 41,000	Bipolar plate	€ 11,211
Tank	€ 9082	Felt electrode	€ 11,047
System assembling	€ 9000	Frame	€ 3066
Power electronics	€ 5000	Membrane	€ 6656
Fluid components	€ 3420	Gasket	€ 16,974
Control engineering	€ 9160	Assembling	€ 2782
VRFB stack	€ 52,646	End plate	€ 435
VRFB stack specific cost	€ 5265 /kW	Isolation plate	€ 217
Total system cost	€ 129,310	Current collector	€ 141
Total system specific cost	€ 1078 / kWh	Connection	€ 119

Table 2.
Cost analysis of 10 kW/120 kWh VRFB system. Reproduced with permission from [32]. Copyright 2016 by Noack J. et al.
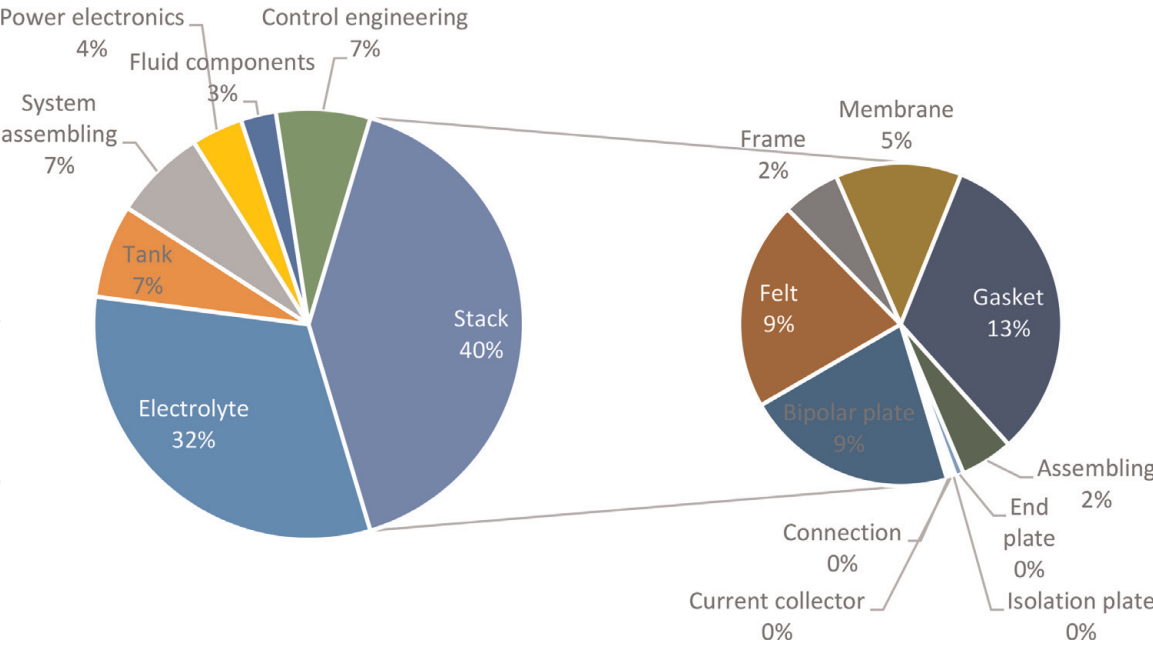
Figure 11.
10 kW/120 kWh VRFB system cost analysis. Reproduced with permission from [32]. Copyright 2016 by Noack J. et al.

the total cost. Electrolyte accounts for 32% of the total cost, which is the largest portion as a single component. In order to increase the energy content of the flow battery, the additional active material and the tank are required, so that the cost proportion of the electrolyte may increase depending on the storage capacity increase and the fluctuation of vanadium market price. In this analysis, the energy storage cost for VRFB system is presented at € 1078/kWh, which is expected to decrease with increasing production quantities.

6. Conclusions

Vanadium redox flow battery is one of the most promising devices for a large energy storage system to substitute the fossil fuel and nuclear energy with renewable energy. The VRFB is a complicated device that combines all the technologies of electrochemistry, mechanical engineering, polymer science, and materials science similar to the fuel cell. To optimize the flow battery design, it is necessary to understand the flow distribution, local current distribution, limits, and maximum current density. Understanding the shunt current and pressure distribution allows to design the flow battery stack with high power, large capacity, and high system efficiencies. Both experimental and modeling approaches are required to develop advanced vanadium redox flow battery stacks with high electrochemical performance.

Since Skyllas-Kazacos group at the University of New South Wales invented the VRFB in 1986, many researchers have conducted VRFB research. It is true that the VRFB are closer to commercialization than any other flow batteries. However still many of the reaction mechanisms and material characteristics must be further studied, and it is sure that the vanadium redox flow batteries are still very attractive research topics.

Acknowledgements

Author details

Sangwon Kim[1,2]

1 Korea Institute of Science and Technology (KIST) Europe, Saarbrücken, Germany

2 Transfercenter Sustainable Electrochemistry, Saarland University, Saarbrücken, Germany

*Address all correspondence to: sangwon.kim@kist-europe.de

IntechOpen

References

[1] Chen R, Kim S, Chang Z. Redox flow batteries: Fundamentals and applications. In: Khalid M, editor. Redox: Principles and Advance Applications. London: InTech; 2017. pp. 103-118. DOI: 10.5772/intechopen.68752

[2] Ye R, Henkensmeier D, Yoon SJ, Huang Z, Kim DK, Chang Z, et al. Redox flow batteries for energy storage: A technology review. ASME Journal of Electrochemical Energy Conversion and Storage. 2018;**15**:010801. DOI: 10.1115/1.4037248

[3] Choi C, Kim S, Kim R, Choi Y, Kim S, Jung H, et al. A review of vanadium electrolytes for vanadium redox flow batteries. Renewable and Sustainable Energy Reviews. 2017;**69**:263-274. DOI: 10.1016/j.rser.2016.11.188

[4] Alotto P, Guarnieri M, Moro F. Redox flow batteries for the storage of renewable energy: A review. Renewable and Sustainable Energy Reviews. 2014;**29**:325-335. DOI: 10.1016/j.rser.2013.08.001

[5] Bard AJ, Faulkner LR. Electrochemical Methods: Fundamentals and Applications. 2nd ed. Hoboken: Wiley; 2000. 832 p

[6] Newman J, Thomas-Alyea KE. Electrochemical Systems. 3rd ed. Hoboken: Wiley; 2004. 647 p

[7] Zhang H, Li X, Zhang J. Redox Flow Batteries: Fundamentals and Applications. Boca Raton: CRC Press; 2018. 432 p

[8] Kim D, Yoon S, Lee J, Kim S. Parametric study and flow rate optimization of all-vanadium redox flow batteries. Applied Energy. 2018;**228**:891-901. DOI: 10.1016/j.apenergy.2018.06.094

[9] Knehr KW, Kumbur EC. Open circuit voltage of vanadium redox flow batteries: Discrepancy between models and experiments. Electrochemistry Communications. 2011;**13**:342-345. DOI: 10.1016/j.elecom.2011.01.020

[10] Hwang G, Kim S, In D, Lee D, Ryu C. Application of the commercial ion exchange membranes in the all-vanadium redox flow battery. Journal of Industrial and Engineering Chemistry. 2018;**60**:360-365. DOI: 10.1016/j.jiec.2017.11.023

[11] Jung M, Lee W, Krishan NN, Kim S, Gupta G, Komsyska L, et al. Porous-Nafion/PBI composite membranes and Nafion/PBI blend membranes for vanadium redox flow batteries. Applied Surface Science. 2018;**450**:301-311. DOI: 10.1016/j.apsusc.2018.04.198

[12] Chen C, Henkensmeier D, Kim S, Yoon SJ, Zinkevich T, Indris S. Improved all-vanadium redox flow batteries using catholyte additive and a cross-linked methylated polybenzimidazole membrane. ACS Applied Energy Materials. 2018;**1**:6047-6055. DOI: 10.1021/acsaem.8b01116

[13] Strużyńska-Pirona I, Jung M, Maljuschc A, Conradic O, Kim S, Jang J, et al. Imidazole based ionenes, their blends with PBI-OO and applicability as membrane in a vanadium redox flow battery. European Polymer Journal. 2017;**96**:383-392. DOI: 10.1016/j.eurpolymj.2017.09.031

[14] Lee Y, Kim S, Hempelmann R, Jang JH, Kim HJ, Han J, et al. Nafion membranes with a sulfonated organic additive for the use in vanadium redox flow batteries. Journal of Applied Polymer Science. 2019;**136**:47547. DOI: 10.1002/app.47547

[15] Ulaganathana M, Aravindan V, Yan Q, Madhavi S, Skyllas-Kazacos M, Lim TM. Recent advancements in all-vanadium redox flow batteries. Advanced Materials Interfaces. 2015;**3**: 1500309. DOI: 10.1002/admi.201500309

[16] Kim KJ, Park MS, Kim YJ, Kim JH, Dou SX, Skyllas-Kazacos M. A technology review of electrodes and reaction mechanisms in vanadium redox flow batteries. Journal of Materials Chemistry A. 2015;**3**:16913-16933. DOI: 10.1039/C5TA02613J

[17] Sum E, Skyllas-Kazacos M. A study of the V(II)/V(III) redox couple for redox flow cell applications. Journal of Power Sources. 1985;**15**:179-190. DOI: 10.1016/0378-7753(85)80071-9

[18] Sum E, Rychcik M, Skyllas-Kazacos M. Investigation of the V(V)/V(IV) system for use in the positive half-cell of a redox battery. Jounral of Power Sources. 1985;**16**:85-95. DOI: 10.1016/0378-7753(85)80082-3

[19] Li L, Kim S, Wang W, Vijayakumar M, Nie Z, Chen B, et al. A stable vanadium redox-flow battery with high energy density for large-scale energy storage. Applied Energy Materials. 2011;**1**:394-400. DOI: 10.1002/aenm.201100008

[20] Ulaganathana M, Jain A, Aravindan V, Jayaraman S, Ling WC, Lim TM, et al. Bio-mass derived mesoporous carbon as superior electrode in all vanadium redox flow battery with multicouple reactions. Jounral of Power Sources. 2015;**15**:846-850. DOI: 10.1016/j.jpowsour.2014.10.176

[21] Park SK, Shim J, Yang JH, Jin CS, Lee BS, Lee YS, et al. The influence of compressed carbon felt electrodes on the performance of a vanadium redox flow battery. Electrochimica Acta. 2014;**116**:447-452. DOI: 10.1016/j.electacta.2013.11.073

[22] Oh K, Won S, Ju H. Numerical study of the effects of carbon felt electrode compression in all-vanadium redox flow batteries. Electrochimica Acta. 2015;**181**:13-23. DOI: 10.1016/j.electacta.2015.02.212

[23] Yoon SJ, Kim S, Kim DK. Optimization of local porosity in the electrode as an advanced channel for all-vanadium redox flow battery. Energy. 2019;**172**:26-35. DOI: 10.1016/j.energy.2019.01.101

[24] Weber AZ, Mench MM, Meyers JP, Ross PN, Gostick JT, Liu Q. Redox flow batteries: A review. Journal of Applied Electrochemistry. 2011;**41**:1137-1164. DOI: 10.1007/s10800-011-0352-6

[25] Leung P, Li X, Leon CP, Berlouis L, Low CTJ, Walsh FC. Progress in redox flow batteries, remaining challenges and their applications in energy storage. RSC Advances. 2012;**2**:10125-10156. DOI: 10.1039/C2RA21342G

[26] Ke X, Prahl JM, Alexander JID, Wainright JS, Zawodzinski TA, Savinell R. Rechargeable redox flow batteries: Flow fields, stacks and design considerations. Chemical Society Reviews. 2018;**47**:8721-8743. DOI: 10.1039/C8CS00072G

[27] Ke X, Alexander JID, Prahl JM, Savinell RF. Flow distribution and maximum current density studies in redox flow batteries with a single passage of the serpentine flow channel. Journal of Power Sources. 2014;**270**:646-657. DOI: 10.1016/j.jpowsour.2014.07.155

[28] Aaron A, Tang Z, Papandrew AB, Zawodzinski TA. Polarization curve analysis of all-vanadium redox flow batteries. Journal of Applied Electrochemistry. 2011;**41**:1175-1182. DOI: 10.1007/s10800-011-0335-7

[29] Aaron DS, Liu Q, Tang Z, Grim GM, Papandrew AB, Turhan A, et al. Dramatic performance gains in

vanadium redox flow batteries through modified cell architecture. Journal of Power Sources. 2012;**206**:450-453. DOI: 10.1016/j.jpowsour.2011.12.026

[30] Elgammal RA, Tang Z, Sun CN, Lawton J, Zawodzinski TA. Species uptake and mass transport in membranes for vanadium redox flow batteries. Electrochimica Acta. 2017;**237**: 1-11. DOI: 10.1016/j.electacta.2017. 03.131

[31] Ha S, Gallagher KG. Estimating the system price of redox flow batteries for grid storage. Journal of Power Sources. 2015;**296**:122-132. DOI: 10.1016/j. jpowsour.2015.07.004

[32] Noack J, Wietschel L, Roznyatovskaya N, Pinkwart K, Tübke J. Techno-economic modeling and analysis of redox flow battery systems. Energies. 2016;**9**:627. DOI: 10.3390/ en9080627